IOP Conference Series:
Materials Science and
Engineering

PAPER • **OPEN ACCESS**

Single sided water absorption in thick GFRP structures: Mechanical effects and diffusion monitoring by integrated smart sensors

To cite this article: Dennis Gibhardt *et al* 2025 *IOP Conf. Ser.: Mater. Sci. Eng.* **1338** 012034

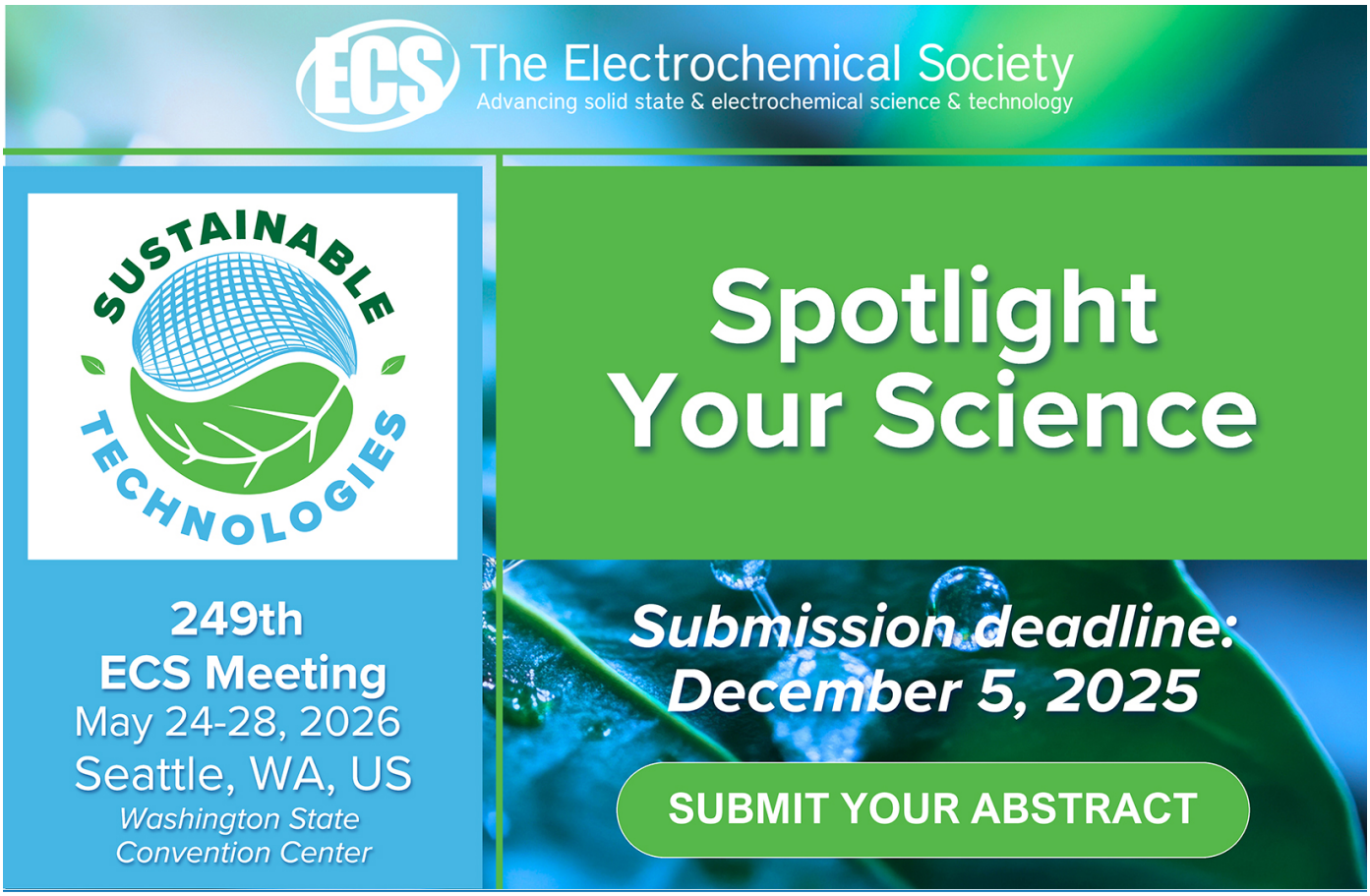

IOP Conf. Series: Materials Science and Engineering **1338** (2025) 012034 doi:10.1088/1757-899X/1338/1/012034

Single sided water absorption in thick GFRP structures: Mechanical effects and diffusion monitoring by integrated smart sensors

Dennis Gibhardt[1], Christina Buggisch[1], Melissa Walter[1], Maximilian Ahrens[1] and Bodo Fiedler[1]

[1]Hamburg University of Technology, Institute of Polymers and Composites, Denickestraße 15, 21073 Hamburg, Germany

E-mail: dennis.gibhardt@tuhh.de

Abstract. In many application scenarios, such as the wind energy industry, fibre-reinforced polymers undergo atmospheric ageing due to prevailing environmental conditions. As a result, moisture gradients are often present in the material, which influence the material behaviour and mechanical properties. Reliable determination of the current moisture condition at various points in the component and knowledge of the effects of moisture on the mechanical behaviour of the structure can extend the service life and prevent failure. Consequently, this work presents a method for monitoring local moisture absorption and moisture-induced damage in thick GFRP laminates. Therefore, an integrated sensor system based on single carbon fibre (CF) rovings and impedance measurements was developed. Water absorption leads to a change in the dielectric properties of the GFRP, resulting in a significant increase in the phase angle and a simultaneous decrease in the amplitude of the electrical impedance, especially when local fibre-matrix debonding occurs. In addition, the mechanical effects of non-symmetric water absorption are evaluated using four-point bending and interlaminar shear strength tests. The mechanical performance of the aged laminates decreased significantly, even though the water infiltrated the laminates by less than 25 % of the thickness.

1 Introduction

The ageing of polymer composites is an important issue in many applications, such as the offshore, marine, or wind energy industries, because the structures are exposed to harsh environmental conditions for decades. Typically, moisture gradients develop from the surfaces in contact with moisture or water into the composite material (see Figure 1). The underlying diffusion process depends on the ambient temperature and the specific material selection, whereby fibre-reinforced polymers (FRPs) often exhibit approximately Fickian diffusion behaviour. Long-term predictions are typically based on isothermal ageing tests, accelerated by immersing coupons in water at temperatures higher than the service temperature [1, 2]. Design parameters are derived from small-scale coupon tests on saturated specimens. However, for FRP structures of several millimetres thickness under real operating conditions, it takes years or even decades for the laminates to become fully saturated. Since it is well known that especially glass fibre-reinforced polymers (GFRPs) can experience significant reductions in mechanical properties due to moisture absorption [3, 4], a reliable determination of the current moisture condition at various points in the structures is beneficial.

Furthermore, there is an ongoing discussion about the effects of the ageing conditions on the results received with coupon testing compared to more application-oriented scenarios [5]. In detail, there is still the question of the extent to which the immersion of coupons with open cutting edges affects the results because of the easy access of water to the fibres and the fibre-matrix interphases. Even though it is readily investigated that the water absorption along the fibre direction within the fibre-matrix interphase is about two to four times faster than in the (normal) thickness direction [6, 7], it is not clear yet if the closed matrix surface effectively protects fibres from damage during a single-sided diffusion process.

To gain more insight into the actual material state of thick GFRP structures, in-situ and in-depth monitoring is needed. As a non-destructive testing approach, electrical measurements can be used as easy and affordable structural health monitoring (SHM, see Figure 1) [8]. Compared to resistance measurements, capacitance or electrical impedance measurements allow electric SHM to be performed in

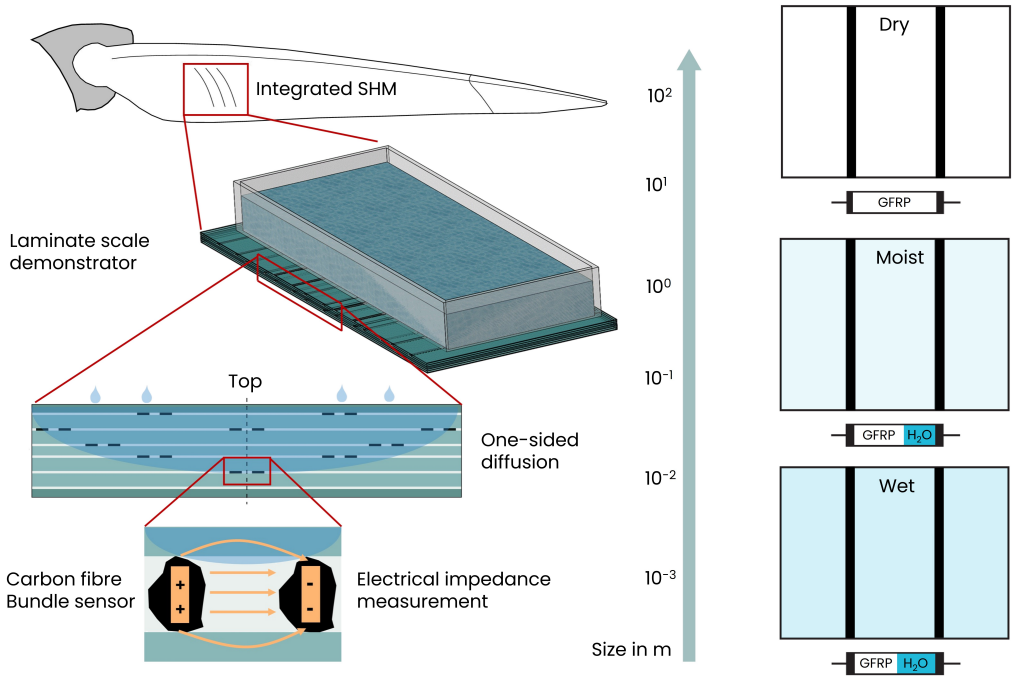

Figure 1: Left: Scheme of the carbon fibre bundle sensor principle at different size scales. Right: Schematic representation of the sensor principle by water-induced permittivity changes.

non-conductive composite materials like GFRP using integrated electrodes or surface electrodes. The detection capability of capacitance-based methods is dependent on a change in the dielectric properties of the material [9]. Generally, all effects that cause a change in the dielectric constant of the material, such as damage and moisture, can be detected with capacitive SHM. Today, impedance or capacitance measurements are used to detect voids and damage [10, 11], rebar reinforcement corrosion and localisation [12, 13] as well as moisture [14, 15] in concrete structures. In capacitive imaging, pairs of coplanar electrodes without surface contact are used to scan a surface and measure changes in charge for specific voltages, providing a map of changes in electrical properties that can detect cracks, voids or moisture [16]. However, for polymers or FRPs, research on capacitance or impedance measurements for damage detection is limited. Chakraborty et al. [17, 18] have used capacitance measurements to detect stresses and defects between layers in 3D printed polymers. Similar to concrete, capacitive imaging with non-contact coplanar electrodes can be used to detect and locate moisture or damage in various FRP composites such as CFRP [19, 20] or GFRP [21, 22].

Structural integration without significant changes in the mechanical properties can be achieved when GFRPs are modified with carbon nanoparticle (CNP)-filled (thermoset) films as strain sensors, like published in [23] or with the implementation of carbon fibre bundles as capacitors. Forintos et al. [24] proved the possibility of resistive strain monitoring on embedded CF bundles in GFRP, while Buggisch et al. [25] reported the transfer to impedance measurements.

2 Materials and methods

2.1 Manufacturing

For the present study, laminates with a $[\pm 45_2/90_2/0_3/90_2/0_3/90_2/0_2]_s$ lay-up and a total thickness of 9.2 mm were manufactured in a resin transfer moulding process. In 0° direction, a unidirectional fabric UNIE400 (SELCOM SRL) with an areal weight of 400 $\mathrm{g\,m^{-2}}$ was used. The ±45° layers consisted of bi-axial fabrics G300BX (HACOTECH) with an aerial weight of 300 $\mathrm{g\,m^{-2}}$ and the 90° layers of unidirectional fabrics UT-ET250 (Gurit) with a serial weight of 250 $\mathrm{g\,m^{-2}}$. Single glass fibre bundles of the 90° layers were replaced with carbon fibre bundles FT300B 6000-50B (Toray Carbon Fibres Europe). Figure 1 shows a schematic representation of the laminate lay-up, including the arrangement of the CF.

The used layers and the nominal laminate thickness lead to a calculated fibre volume content of 46.6 %. The epoxy resin system Hexion EPIKOTE™ Resin MGS™ RIMR 135 and EPIKURE™ Curing Agent MGS™ RIMH 137 with a mixing ratio of 100:30 weight shares, was used for infusion. The laminate was cured in a hot-press for 10 h at 50 °C and post-cured in an oven for 16 h at 80 °C. Each laminate was cut into four pieces of 270x120 mm^2 using an Altendorf F45 saw. Additionally, a 10.0 mm thick pure epoxy plate including CF bundle sensors directly under the surface and in the middle of the thickness was manufactured with the same parameters. This plate was used both to perform absorption, FTIR and impedance experiments.

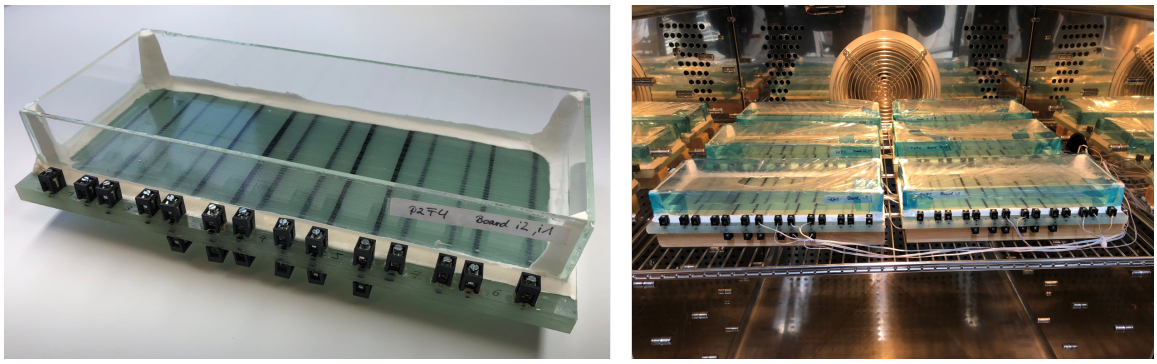

Figure 2: Left: Final assembly of the electrically contacted laminates with water bath for single-sided absorption. Right: Setup in the climate chamber during hygrothermal ageing.

2.2 Hygrothermal ageing and monitoring

For the single-sided hygrothermal ageing process, a glass basin was glued onto each laminate quarter using silicon glue (Knauf). Prior to hygrothermal ageing each laminate quarter was dried for 200 h at 40 °C in a vacuum oven VO 400 (Memmert). Hygrothermal ageing was performed in a climate chamber CTC 256 (Memmert) at a temperature of 50 °C and a relative humidity of 40 %. These conditions were used to accelerate the diffusion process and possibly cause severe damage to the exposed laminate surface below the water basin, but not to the other surfaces in the climate chamber. The main and single-sided water uptake was realised by filling the glass basins with 50 °C warm, demineralised water. The electric conductivity of the demineralised water was measured as 2.6 $\mu S\,cm^{-1}$. To avoid evaporation, the glass basins were covered with PE foil and sealed with adhesive tape. Figure 2 shows a photo of a fully prepared laminate quarter and the arrangement inside the climate chamber with full wiring.

The accompanying thick epoxy resin plate was also fitted with a water-filled glass frame to monitor the moisture distribution inside the samples by continuous impedance measurements and subsequent FTIR analysis of thin sections. However, the relative humidity was 70 % in this case. After six months, the frame was removed, and a 0.3 mm thin section was cut from the centre of the sample. The thin section was placed directly into the FTIR microscope, and 100 measurements were taken along a line from the top to the bottom of the sample. The total processing time was $\leq$ 10 min, which was sufficient to minimise drying. The FTIR spectra were analysed at the 5238 cm^{-1} peak, which is known to be directly related to water inside the epoxy as described in [26]. In addition, strips cut from the samples prepared in the same way and stored at room temperature and 50 % relative humidity were examined for the same period. The peak areas were converted into percentages of the absorbed mass according to the relation described in Gibhardt et al. [27]. As shown in Figure 3, the peak integral A_I increases linearly with water absorption (measured gravimetrically) and, therefore, allows the determination of the local in-depth water amount M_t by FTIR measurements. The relation can be described as:

$$M_t = \frac{A_I - 0.2}{10.8}, \tag{1}$$

To avoid further ageing effects during water absorption, calibration measurements were performed by ageing in 8 °C water.

To perform impedance measurements during hygrothermal ageing, the laminate quarters were contacted. Therefore, 1.2 mm holes were drilled in the GFRP laminates at the positions of the CF bundles,

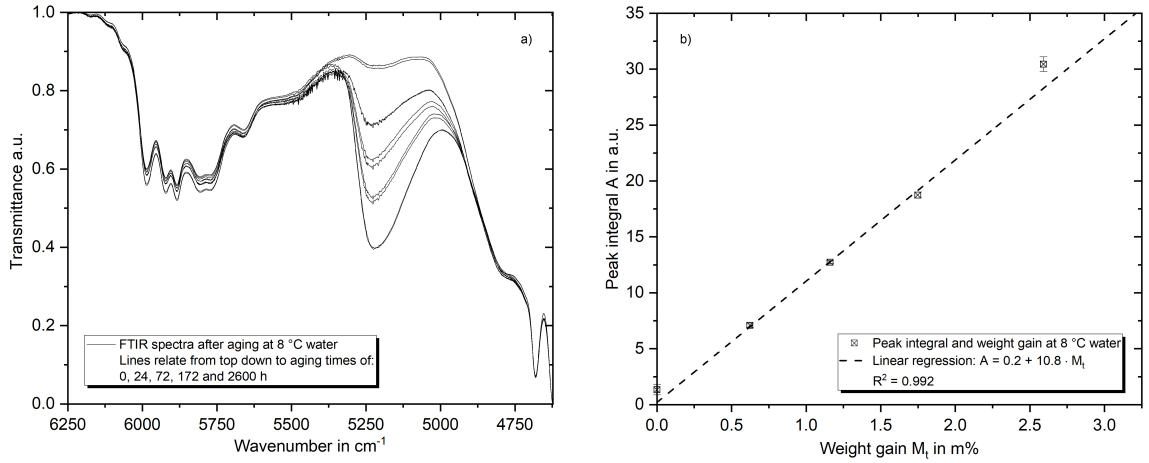

Figure 3: Left: FTIR-spectra around the peak of 5238 cm^{-1} of the RIMR135/H137 epoxy during ageing at 8 °C water until saturation. Right: High correlation between the peak integral and the weight gain. From Gibhardt et al. [27].

filled with Acheson 1415 silver conductive paint and one pin screw clamps were attached and fixed in place using epoxy resin system Hexion EPIKOTE™ Resin MGS™ RIMR 135 and EPIKURE™ Curing Agent MGS™ RIMH 134.

Impedance measurements were performed using a low-cost measurement board consisting of an impedance measurement board Digilent PmodIATM, a Wemos D1 mini microcontroller (MC) for wireless transfer of measurement data, an 8-channel multiplexer Nexperia 74HC4051 and a resistance used for calibration. A constant voltage source 3234 (Statron) was supplying a constant voltage of 5 V. Impedance measurements can be performed in the range of 100 Ω to 100 MΩ with frequencies of 1 kHz to 100 kHz. One measurement board can measure seven electrode pairs. Five measurement boards were used. A frequency of 10 kHz was used for all measurements as the best sensitivity was achieved for this frequency in prior tests [25].

2.3 Mechanical testing

Mechanical tests were performed on a Zwick 10 kN universal testing machine. At different times during hygrothermal ageing, the glass basins were carefully removed from the laminate quarters. Specimens for four-point bending (4-PB) and interlaminar shear strength (ILSS) tests were cut using a Brillant 265 saw (ATM Germany). Additionally, some pieces for re-drying were cut to determine the moisture content in the laminate. Each laminate quarter consisted of four 4-PB specimens, three ILSS specimens and four re-drying specimens. The 4-PB specimens had a size of 270x15x9.2 mm^3. The ILSS specimens were 55.5x15.5x9.2 mm^3 big and the re-drying specimens 10x15.5x9.2 mm^3.

ILSS tests were performed according to ASTM D2344 with a speed of 1 mm min^{-1}. A support distance of 36 mm, diameter of the lower support of 4 mm and diameter of the upper roller of 6 mm were used.

4-PB tests were performed according to DIN EN ISO 14125. Tests were performed with 5 mm min^{-1} test speed and a roller diameter of 10 mm. The outer support width was 100 mm and the inner support width was 69 mm. The edge fibre elongation was measured using an inductive displacement transducer and an MGC measuring amplifier (Hottinger Baldwin Messtechnik).

In addition, a digital image correlation system Aramis 4m (GOM GmbH) was used for strain measurements during some tests. In both tests, the specimens were differentiated whether the exposed area was above and subjected to compression (WCS) or below and subjected to tensile stress (WTS). Re-drying of specimens was performed in a VO 400 vacuum oven (Memmert) at 40 °C. Weight measurements of the samples were taken before drying and at specific time intervals.

3 Results and discussion

3.1 Water absorption and FTIR-analysis

Figure 4 shows the amount of water absorbed locally through the thickness of the pure epoxy plate after storage in the climate chamber. The calculated values based on the FTIR technique correspond well to the expected values for immersion in 50 °C water (exposed surface at distance 0), as well as the saturation value of about 1.45 m% at 50 °C and 70 % RH. Furthermore, the water absorption of 0.95 m% under laboratory conditions corresponds well to the results obtained with gravimetric measurements. However, the amount of about 3.75 m% on the surface exposed to water seems to be a bit too high. The measurements along a line through the thickness also reveal the water distribution, which follows a Fickian trend from the equilibrium of the water contact site to the equilibrium at the humid surface. Finally, it can be concluded that the trough-thickness FTIR analysis used is suitable to be used for the calibration of any electrical measurements, such as the proposed continuous impedance measurements. To do this, the electrical measurements would have to be compared with the FTIR measurements over time.

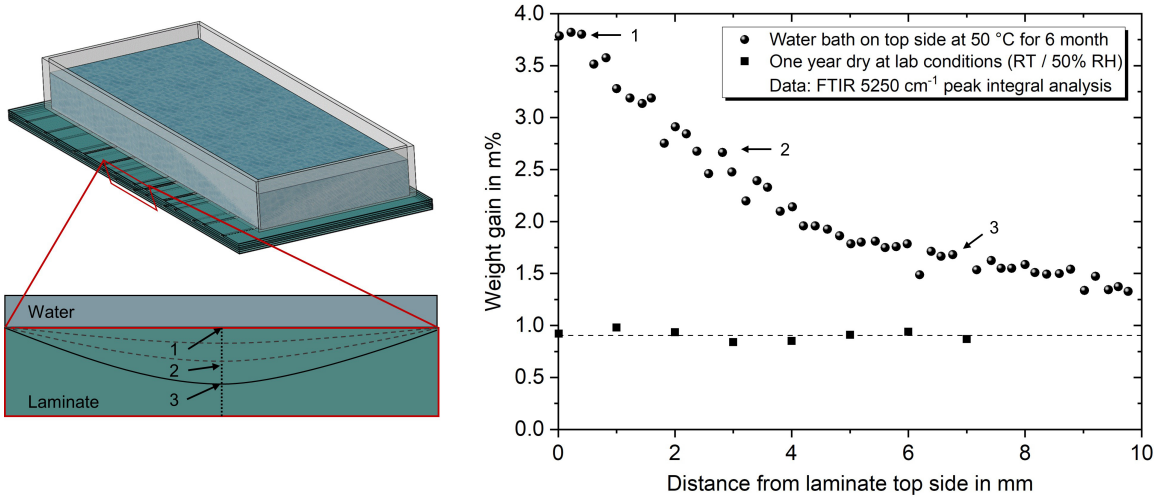

Figure 4: Measurement of the water distribution in a 10 mm thick epoxy plate after one-sided diffusion at elevated temperatures for six months. From Gibhardt et al. [27].

3.2 Continuous impendance measurements

The response of the developed CF sensor design to water contact, absorption, and temperature changes is tested with modified dry fibre fabrics and the pure resin plate first. When the dry fabric is immersed in water, a significant and instantaneous change of impedance magnitude $|Z|$ and phaseangle φ_z occurs. After a few minutes, the drop of magnitude becomes stable with a permanent relative change of about 80 %, while the phaseangle changes by about 70 %. Consequently, these values describe the maximum changes to be expected when water is the surrounding medium instead of air. In practical applications, the expected change is correspondingly lower because the permittivity of GFRP only changes because of water absorption. Greater changes are only expected when large amounts of water accumulate as clusters in free spaces. By recording the impedance $|Z|$ and phaseangle φ_z for the epoxy plate before, during, and after filling the water tank on the upper side, it is possible to determine the influence of the ambient medium on the measurement. Due to the water load, $|Z|$ drops abruptly by about 30 % while φ_z increases by about 10 %. This effect can be attributed to the sudden change in the complex permittivity of the dielectric. Due to proximity to the diffusion medium and the formation of a presumably inhomogeneous field-line distribution, changes in dielectric properties are also detected near the electrode pair. Finally, the effects of an increase in temperature from room temperature to 50 °C were found to be small with no significant change in $|Z|$ and a stable decrease of φ_z by 2.5 %. Consequently, the long-term measurements on the GFRP laminates and epoxy plate were started after the water filling and temperature homogenisation inside the climate chamber.

In contrast to what was expected, a 30-day single-sided water absorption in the pure epoxy plate did not significantly change the measured impedance $|Z|$ and phaseangle φ_z, even though the global amount of absorbed water after that time was more than 1.4 m% (measured gravimetrically by desorption). On the one hand, this could be a consequence of a non-ideal measuring setup, too small absolute capacities, a non-ideal frequency [9] and too large noise. However, a similar result was previously described by Fukuda et al. [28]. The authors found that the change in dielectric properties with water absorption was insignificant for a pure epoxy, whereas a similar epoxy filled with silica powder particles showed a two-fold increase in the relative permittivity during the same absorption period. They concluded that the particle-matrix interphase is filled with water and thus, polarisation at the interface is decisive. In contrast, the distributed water molecules within the matrix molecule network have only a limited impact.

In Figure 5, the continuous measurement of the impedance $|Z|$ and phaseangle φ_z of a representative GFRP laminate is displayed for the upper two sensor levels over more than 280 days. The sensor layers three to five are not shown, as these do not differ from the second sensor level. It is clear to see that the measurements in the first sensor level (0.7 mm below the surface) and the second sensor level (2.3 mm below the surface) differ significantly. While for the first sensor layer both $|Z|$ and φ_z change continuously and significantly by up to 21 % and 12 %, respectively, the maximum relative changes in the second layer are about 3 %.

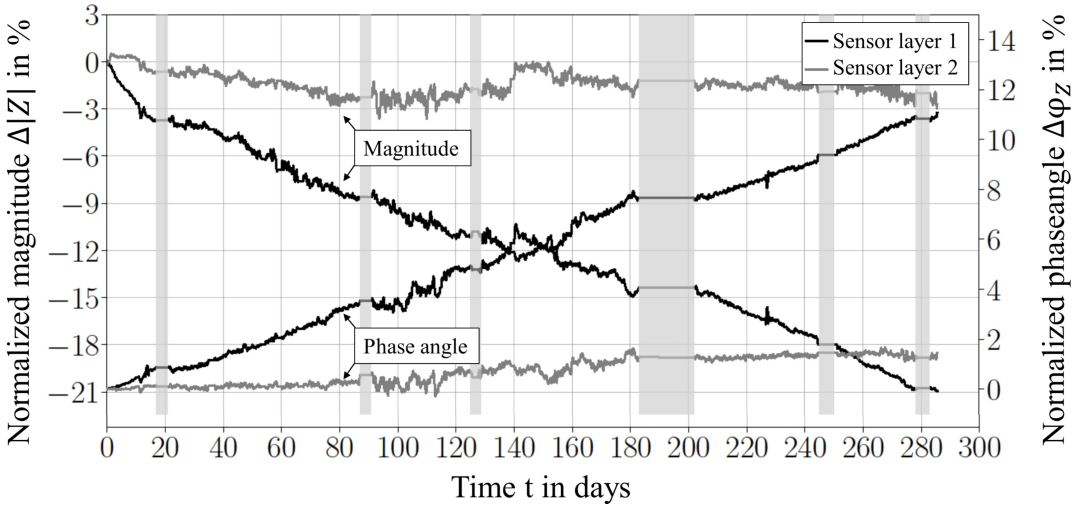

Figure 5: Development of magnitude $|Z|$ and phaseangle φ_z for two sensor layers. Grey bars indicate breakdowns of the measuring system due to shutdowns.

Taking the tests on the pure epoxy plates into account, it is hypothesised that the water absorption effect of the matrix cannot explain the results gained with the first sensor layer. Instead, after a short time, the first fibre-matrix debondings could already be detected visually within the first two laminate layers. These debondings grow and increase progressively in quantity during the ageing test. A photograph of the surface after 400 days, showing the large number of fibre-matrix debondings before mechanical testing, is displayed on the right side of Figure 6. However, as these severe interphase damages are limited to the uppermost laminate layers for the majority of the test duration, it can be explained why the sensors in the lower layers did not show significant changes. In conclusion, this means that continuous measurements of impedance magnitude $|Z|$ and phaseangle φ_z using CF bundle sensors in several GFRP laminate layers allow local detection of severe fibre-matrix damage caused by water absorption. The water absorption itself or the specific amount of water through the thickness could not be detected with certainty, as the measurement noise was large, and the absolute change of permittivity due to water absorption in the matrix seems to be small compared to the effects of water clusters within damaged (interphase) regions. In conclusion, the insensitivity to pure moisture absorption in the matrix resin is even positive for SHM applications, as it allows clear assignment of measurement data to the type of damage described. Furthermore, FTIR measurements reveal that the single-sided water absorption follows well the expected Fickian behaviour and is, therefore, easily predictable.

For future studies and the application in the field, the adjustable sensor design (distance and cross-sectional area) allows an adaptation of the sensitivity and measurement scale to the real composite

part and the used equipment. Furthermore, sensors can be used for multiple tasks, from manufacturing (degree of curing state) to operation (media absorption and damage detection), as described by Buggisch et al. [25, 29].

3.3 Impact on mechanical properties

The results of the 4-PB tests and the ageing damage of the water-stressed surface are summarised in Figure 6. It can be seen that the flexural strength of the laminates decreases continuously. After 400 days of exposure, the strength reduction was 25 % when a tensile load was applied and about 17 % when a compression load was applied to the exposed laminate side. Taking into account the results of the impedance measurements and the laminate layup, it is noticable that the magnitude of strength loss matches the assumption of only the upper 25 % of the laminate being affected by severe fibre damage. This is because the depth of ageing dependent fibre-matrix debondings is limited to the first layers of 0°-fibres. Compared with studies on similar materials, this is within a fairly accurate range predicted from the short-term ageing tensile tests described in [27] after ageing at 50 °C when the thickness of the laminate is taken into account. In addition, the typical damage and fracture pattern changed continuously. As the dry and short-term aged specimens regularly fractured through delamination failure below the laminate surface within the 90° layers and through the final compression fracture of the upper ±45° layers, the compression fracture propagated deeper into the composite. This is consistent with previous reports of flexural tests on aged reinforced plastics, e.g. Boisseau et al . [30]. Here, the authors observed a continuous change from compressive to tensile failure, as the reduction in glass fibre strength has a greater effect on the tensile strength than on the compressive strength. As can be seen from the images in Figure 6, the same frequent F/M delamination occurred in the layers near the surface exposed to water as in the GFRP samples after full immersion described in [27, 31, 32]. Consequently, it can be assumed that even a closed matrix surface cannot permanently protect the composite material and especially the fibres from direct contact with water under such harsh conditions as applied with the accelerated ageing tests at 50 °C.

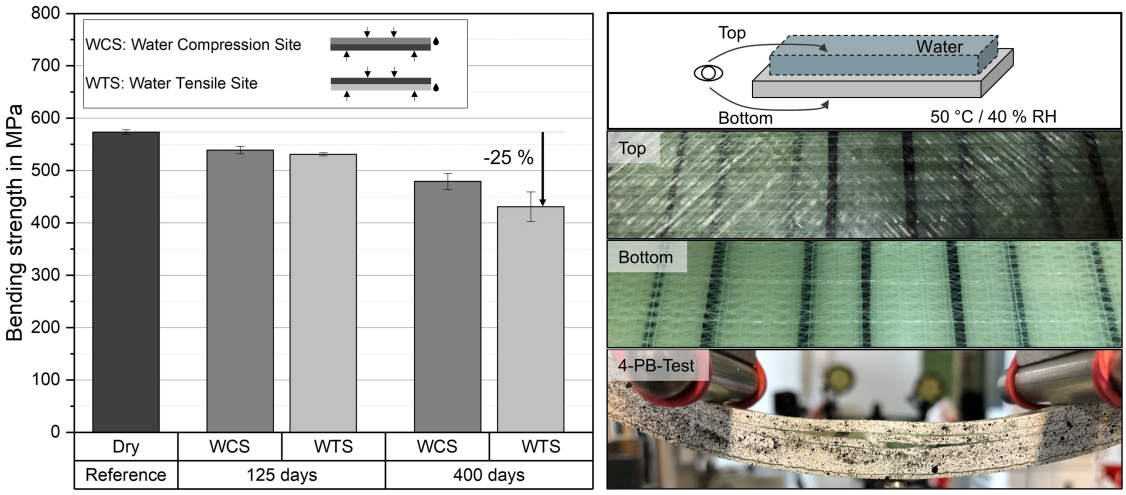

Figure 6: Left: 4-point-bending strength evolution during one-sided water absorption over up to 400 days. Right: Photographs showing fibre-matrix debondings near the exposed surface and the undamaged bottom side before testing, as well as the progressive damage during testing.

Similarly, Figure 7 displays the results of the ILSS tests. These tests were carried out after up to 125 days of single-sided ageing, and again, the exposed side was set under tensile or compression load, respectively. Compared to 4-PB tests, the impact of single-sided ageing on ILSS performance is remarkably lower. While there was no statistically relevant change after 90 days of exposure, the ILSS decreased by about 10-12 % after 125 days. These results are in line with what can be expected, as the test is designed to introduce a maximum shear loading in the symmetry plane of the laminate. Firstly, the plane of symmetry is relatively far away from the exposed surface, and secondly, no F/M debondings

were detected at the corresponding depth. As can be seen from the photograph in Figure 7, the first failure frequently started slightly outside the symmetry plane in the overlying or underlying 90°-layer. Therefore, it is assumed that the shear strength of these layers is lower than the interphase shear strength of the 0°-layers in the symmetry plane. However, the relative strength decreases after 125 days of exposure are reasonable, considering the shear strength reductions of about 20 % found by Gagani et al. [32] and about 40 % by Rocha et al. [31] for fully immersed and saturated GFRP samples.

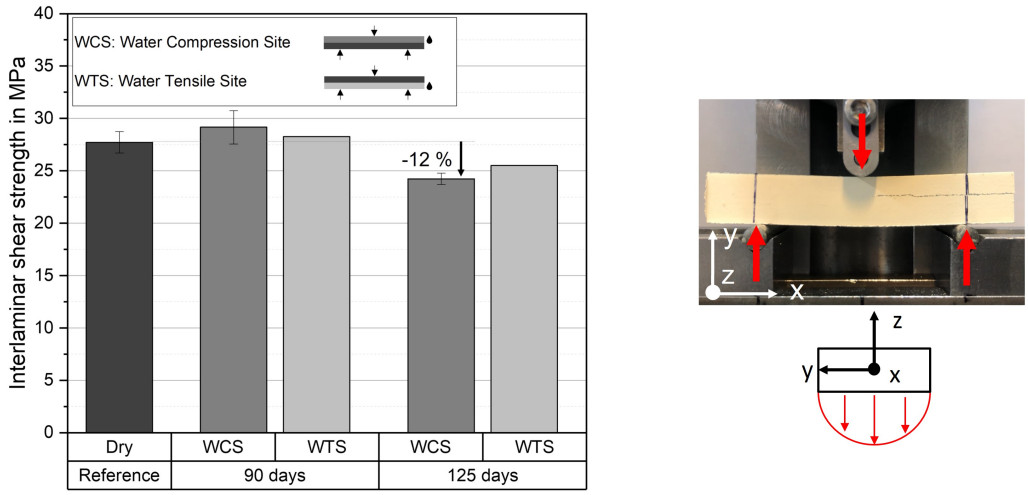

Figure 7: Left: Results obtained in ILSS tests with water exposed surface on compression resp. tensile site. Right: Representative photograph of the ILSS test with a visible crack slightly above the midplane.

4 Conclusion

The presented methodology for in-situ electrical impedance measurements using a newly designed integrated CF bundle sensor enables the local detection of critical F/M debondings caused by moisture in GFRP. These debondings lead to a change in the dielectric properties of the GFRP caused by clustered water, which results in a significant increase in the phase angle and a simultaneous decrease in the amplitude of the electrical impedance. Furthermore, the study highlights the drastic influence of high local moisture content and especially resulting weakening within the F/M interphase on the integrity of thick GFRP structures. Therefore, this study provides a new SHM method and valuable insights for the design of wind turbine blades.

Although the CF bundle sensor could not accurately detect moisture gradients in the material using the chosen measurement setup, electrical impedance measurements are generally a valuable SHM approach for moisture detection. As the bundles only represent small capacitor areas, an extension of the study using, e.g., integrated CNT-modified epoxy film sensors, is conceivable to capture the moisture gradients. A combination of bundle and film sensors promises a comprehensive monitoring method.

Although the global amount of water absorbed was far from saturation, the high local moisture content near the exposed surface caused severe local laminate damage. Under bending loads, the reduced tensile strength of the debonded fibres resulted in a significant loss of strength. In detail, drastic decreases of up to 25 % in 4-PB strength and 12 % in ILSS of thick laminates were measurable after long-term single-sided water absorption. As electrical impedance measurements revealed, F/M debondings were more pronounced within the upper laminate layers for the hygrothermal ageing periods tested, leading to a greater change in 4-PB tests compared to ILSS tests.

References

[1] Gibhardt D, Krauklis A E, Doblies A, Gagani A, Sabalina A, Starkova O and Fiedler B 2023 *Polym. Test.* **118** 107901 ISSN 01429418
[2] Chen Y, Davalos J F and Ray I 2006 *J. Compos. Constr.* **10** 279–286
[3] Davies P, Mazeas F and Casari P 2001 *J. Compos. Mater.* **35** 1343–1372
[4] Gibhardt D, Doblies A, Meyer L and Fiedler B 2019 *Fibers* **7** 55
[5] Zhao Y, Li Q, Zhou G, Zhu K, Jing B, Zhu K, Shi J and Li C 2024 *Polymers* **16** 3433
[6] Gagani A I, Krauklis A E and Echtermeyer A T 2018 *Composites, Part A* **115** 196–205
[7] Rocha I B C M, Raijmaekers S, Nijssen R, Van Der Meer F and Sluys L 2016 Experimental/numerical study of anisotropic water diffusion in glass/epoxy composites *IOP Conference Series: Materials Science and Engineering* vol 139 (IOP Publishing) pp 012044
[8] Augustin T, Karsten J, Kötter B and Fiedler B 2018 *Composites, Part A* **105** 150–155
[9] Grammatikos S A, Ball R J, Evernden M and Jones R G 2018 *Composites, Part A* **105** 108–117
[10] Nassr A A and El-Dakhakhni W W 2009 *J. Compos. Constr.* **13** 486–497 ISSN 19435614
[11] Yan J, Downey A, Cancelli A, Laflamme S, Chen A, Li J and Ubertini F 2019 *Sensors* **19** 1843
[12] Cheng Y, Gao F, Hanif A, Lu Z and Li Z 2017 *Constr. Build. Mater.* **149** 659—668 ISSN 0950-0618.
[13] Cheng Y, Hanif A and Li Z 2018 Development of a flexible capacitive sensor for concrete structure health monitoring *Sensors and Smart Structures Technologies for Civil, Mechanical, and Aerospace Systems* vol 10598 (SPIE) pp 154—162
[14] Hudec P, MacInnis C and Moukwa M 1986 *Cem. Concr. Res* **16** 481—490 ISSN 0008-8846
[15] Nassr A A and El-Dakhakhni W W 2008 *Meas. Sci. Technol.* **19** 075702
[16] Yin X, Hutchins D A and Diamond G Gand Purnell P 2010 *Cem. Concr. Res.* **40** 1734–1743 ISSN 0008-8846
[17] Chakraborty P, Gundrati N B, Zhou C and Chung D D L 2017 *Sens. Actuators, A* **263** 380—385 ISSN 0924-4247
[18] Chakraborty P, Zhao G, Zhou C and Chung D D L 2018 *Smart Mater. Struct.* **27** 115012
[19] Diamond G G, Hutchins D A, Gan T H, Purnell P and Leong K K 2006 *Insight - NDT and CM* **48** 724—-730 ISSN 13542575
[20] Gupta S, Kim H E, Kim H and Loh K J 2020 *Meas. Sci. Technol.* **32** 024010 ISSN 0957-0233
[21] Yin X and Hutchins D A 2012 *Composites, Part B* **43** 1282—1292 ISSN 13598368
[22] Amato S, Hutchins D, Yin X, Ricci M and Laureti S 2021 *NDT & E Int.* **124** 102547
[23] Buggisch C, Gibhardt D, Felmet N, Tetzner Y and Fiedler B 2021 *Composites, Part C: Open Access* **6** 100191 ISSN 2666-6820
[24] Forintos N, Sarkadi T and Czigany T 2021 *Compos. Commun.* **28** 100913 ISSN 24522139
[25] Buggisch C, Gibhardt D, Kern M and Fiedler B 2022 *Compos. Commun.* **30** 101090 ISSN 24522139
[26] Capiel G, Uicich J, Fasce D and Montemartini P E 2018 *Polym. Degrad. Stab.* **153** 165–171
[27] Gibhardt D 2024 *Environmental Effects on Composites Durability with regard to Fibers, Matrix, and Interphase* Ph.D. thesis Hamburg University of Technology
[28] Fukuda A, Mitsui H, Inoue Y and Goto K 1997 The influence of water absorption on dielectric properties of cycloaliphatic epoxy resin *Proceedings of 5th International Conference on Properties and Applications of Dielectric Materials* vol 1 (IEEE) pp 58–61
[29] Buggisch C, Gagani A and Fiedler B 2021 *Funct. Compos. Mater.* **2** 1–13
[30] Boisseau A, Davies P and Thiebaud F 2012 *Appl. Compos. Mater.* **19** 459—473
[31] Rocha I, van der Meer F, Raijmaekers S, Lahuerta F, Nijssen R, Mikkelsen L P and Sluys L 2019 *Eur. J. Mech. A. Solids* **73** 407–419
[32] Gagani A I, Krauklis A E, Sæter E, Vedvik N P and Echtermeyer A T 2019 *Compos. Struct.* **220** 431–440